Double-observer approach with camera traps: Towards an unbiased density estimation of unmarked animal populations

Running headline: Estimating the sensitivity of camera traps

Yoshihiro Nakashima[1*], Shun Hongo[2], Kaori Mizuno[2], Gota Yajima[1], Zeun's C.B. Dzefck[3]

[1]College of Bioresource Science, Nihon University, 1866 Kameino, Fujisawa, Kanagawa 252-0880, Japan

[2]The Center for African Area Studies, Kyoto University, 606-8501, Japan

[3]Projet Coméca, Cameroon

[*]Correspondence author. E-mail: yosshi1215jp@yahoo.co.jp

Abstract

1. Camera traps are a powerful research tool with a wide range of applications in animal ecology, conservation, and management. However, camera traps may not always detect animals passing in front, and the probability of successfully detecting animals (i.e. camera sensitivity) may vary spatially and temporarily. This constraint may create a substantial bias in estimating critical parameters, such as the density of unmarked populations or animal activity levels.

2. We applied the 'double-observer approach' to estimate detection probability and correct potentially imperfect detection. This involved two camera traps being set up at a camera station to monitor the same focal area. The detection probability and the number of animal passes were concurrently estimated with a hierarchal capture-recapture model for stratified populations using a Bayesian framework. Monte Carlo simulations were performed to test the reliability. We then estimated the detection probabilities of a camera model (Browning Strike Force Pro) within an equilateral-triangle focal area (1.56 m^2) for 12 ground-dwelling mammals in Japan and Cameroon. We also evaluated the possible difference in detection probability between daytime and nighttime by incorporating it as a covariate.

3. We found that the double-observer approach reliably quantifies camera sensitivity and provides unbiased estimates of the number of animal passes, even when the detection probability varies among animal passes or camera stations. The camera sensitivity did not change between daytime and nighttime either in Japan or Cameroon, providing the first evidence that the number of animal passes per unit time may be a viable index of animal activity levels. Nonetheless, the camera traps missed animals within the focal area by 4 %–36%. Current density estimation models relying on perfect detection may underestimate animal density by the same order of magnitude.

4. Our results showed that the double-observer approach might be effective in correcting imperfect camera sensitivity. The hierarchical capture-recapture model used here can estimate the distribution of detection probability and the number of animals passing concurrently, and thus, it is easily incorporated in the current density estimation models. We believe that this approach could make a wide range of camera-trapping studies more accurate.

Keywords: animal density, camera trap, capture-recapture, detection probability,

double-observer survey, trapping rate, unmarked population

Introduction

Camera trapping is an innovative research technique and has numerous advantages over classic approaches based on human observations. For example, this technique is minimally invasive for animals and habitats and can efficiently collect quantitative records of ground-dwelling mammals, even elusive and nocturnal species, with relatively low labour costs (Silveira et al., 2003; Burton, 2012; Nakashima, 2015). Moreover, by combining it with well-established statistical approaches (Royle & Dorazio, 2008; MacKenzie et al., 2017), wildlife occupancy can be reliably estimated (Linkie et al., 2007; Tobler et al., 2009), abundance or density determined (Karanth, 1995; Royle et al., 2009; Gardner et al., 2010), and species richness assessed (Rovero et al., 2014; Tobler et al., 2015; Li et al., 2018). Furthermore, commercially available camera traps are becoming cheaper, and their battery duration has also been improving (Rovero et al., 2013), allowing for large-scale surveys in space and time (e.g. Norouzzadeh et al., 2018; Nakashima et al., 2020). Data processing (e.g. species identification) may require a long time and heavy labour costs, but a novel technology using machine learning may drastically reduce the cost (Norouzzadeh et al., 2018; Tabak et al., 2019; Willi et al., 2019). Given that camera trapping will be increasingly used to make critical decisions on wildlife conservation management, researchers must

refine this technique further to avoid arriving at an erroneous conclusion.

One of the primary concerns regarding the application of camera traps may be that they may not always detect animals passing within the camera detection zone (i.e. imperfect detection) (Rowcliffe et al., 2011). Studies have shown that camera sensitivity may be primarily a function of animal body mass (e.g. Rowcliffe et al., 2011; Randler & Kalb, 2018). It may be also affected by many factors, such as other animal traits (e.g. typical behaviours), environmental conditions (e.g. temperature and vegetation), and camera efficiency (e.g. trigger speed) (Damm et al., 2010; Driessen et al., 2017; Apps & McNutt, 2018; Jacobs & Ausband, 2018; Randler & Kalb, 2018; Hofmeester et al., 2019; Findlay et al., 2020; McIntyre et al., 2020). This constraint is the reason why the number of animal passes captured by camera traps per unit time (i.e. trapping rate) does not always correlate with animal density and cannot be a reliable index of animal abundance (Sollmann et al., 2013). A series of statistical models are available to account for imperfect detections and reliably estimate animal occupancy and abundance (e.g., MacKenzie et al., 2017). Nonetheless, researchers cannot help assuming perfect or equal detectability in other situations. In particular, although researchers have proposed several analytical approaches to estimate animal density without recognising animal individuals (Rowcliffe et al., 2008; Chandler & Royle, 2013; Ramsey et al., 2015; Howe

et al., 2017; Campos‐Candela et al., 2018; Moeller et al., 2018; Nakashima et al., 2018; Gilbert et al., 2020; Luo et al., 2020; Nakashima et al., 2020), all of these models, except for Chandler and Royle (2013) and Ramsey et al. (2015), assume that camera traps can detect animals passing in a specific area within the camera detection zone with absolute certainty (i.e. perfect detection). Rowcliffe et al. (2011) suggested that the effective area of the camera detection zone (codeterminants of the camera sensitivity) can be determined using a distance sampling approach by applying detection function models to data on the position where animals were first detected. Although this approach is an important step in quantifying camera sensitivity, it also requires perfect detection at a given point within the camera detection zone, which is still questionable. In addition, many studies have estimated the temporal changes in animal activity levels using trapping rates in a given time zone. Indeed, a change in trapping rates within a day should reflect the proportion of animal individuals being active (see Rowcliffe et al., 2013). However, this approach is valid only when the detection probability does not vary (i.e. equal detectability) across time within a day.

A possible yet untested approach to correcting imperfect detection would be to apply the ‘independent multiple observer approach.’ This approach has been used in point-count surveys based on direct observations by human observers (Nichols et al.,

2000; Alldredge at al., 2006; Kissling & Garton, 2006; Riddle et al., 2010; Suryawanshi et al., 2012). In this approach, two or more observers (camera traps in our context) record animals concurrently and independently, and the detection probability is estimated from the match or mismatch of observation records. Two analytical models, the capture-recapture and *N*-mixture models, can be applied to correct imperfect detections (Nichols et al., 2000). The former requires that the observers confer with each other regarding each observation on each count, while the latter may be based solely on the counts from each observer point. Nichols et al. (2000) applied these two models to bird surveys and reported that both models have potential, while the precision of estimates was higher in the former approach. Given that timestamps within images captured by camera traps would allow for efficient reconciling of each count, the capture-recapture model may provide a reliable and efficient means to obtain unbiased estimates of trapping rates. In particular, the hierarchical capture-recapture model using the Bayesian framework is flexibly incorporated into existing density estimation models for unmarked populations.

In this study, we tested the potential of hierarchical capture-recapture models using the Bayesian framework to correct imperfect detections and estimate the number of animal passes. Firstly, we introduced the hierarchical capture-recapture model for

stratified populations proposed by Converse and Royle (2012). Secondly, Monte Carlo simulations were performed to evaluate the effectiveness of this approach. Thirdly, we applied the models to the datasets obtained from two different habitats, Cameroon and Japan, and quantified the detection probability of 12 mammals with varying body sizes. In field applications, we tested whether the time zone might affect detection probability to validate the applications to estimate animal activity levels. We recognise that the double-observer approach may estimate animal density by dividing the expected number of animal passes within a focal area by the size of the focal area; however, we believe that this approach still has several critical constraints as a density estimation model (e.g. variance estimations and model selections). Therefore, in this study, we focused on obtaining a reliable estimate of trapping rates, which is commonly used in current density estimation models for unmarked populations.

Materials and Methods

Model framework

The capture-recapture model applied here is the hierarchical model for stratified populations proposed by Converse and Royle (2012). In the past, it was common to take a two-step approach to the estimation of variations in local population size (i.e. the

number of animal passes at a camera station in our context), N, among populations, obtaining estimates of N using such capture-recapture methods, and then regarding these estimates as data in a second-stage procedure. The advantage of the approach by Converse and Royle (2012) can, unlike traditional approaches, estimate detection probability and population size concurrently. This model can be implemented as follows.

Let us take the individual detection histories y_i (i = 1, 2, …, n) (i.e. the number of camera traps successfully detecting animal passes) from all the S camera stations. Then, let us use a vector, g_i, which denotes the camera station detecting animal passes (referred to as station identity). The number of animal passes at station s can be assumed to flow an arbitrary probability distribution for non-negative integer observations (e.g. Poisson or negative binomial distributions). Here, we assume that the number of animal passes at station s follows a negative binomial distribution with a mean parameter λ_s and dispersion parameter α (which should be more realistic than a Poisson distribution in camera trapping data). The negative binomial distribution is equal to the Poisson distribution with parameter λ_s following a gamma distribution (i.e. gamma–Poisson mixed distribution). Then, a station identifying g_i can be modelled such that:

$$g_i \sim \text{Categorical}\ (\pi)$$

where $\pi = (\pi_1, \pi_2, \ldots \pi_S)$ and $\pi_s = \frac{\eta_s \lambda_s}{\sum_s \eta_s \lambda_s}$ where η_s is the noise term that follows a gamma distribution.

The detection history y_i given by the vector of detection frequencies can be modelled as follows. Because the total population size, N, is unknown, the dimension of the parameter space is also not fixed. To counter this challenge, a data augmentation procedure can be used (Royle & Dorazio, 2012). Specifically, the original detection history of pooled data is artificially augmented by a large number of $M - n$ passes that have all-zero histories (i.e. not detected by either camera). The augmented data will consist of the passes that occurred but were detected by neither camera (false zero), which occurs with probability ψ, and the passes that did not actually occur (structural zeros) with the probability 1 - ψ. A set of latent augmentation binary variables, z_1, $z_2, \ldots z_M$, is introduced, which denotes the false zero (z = 1) and the structural zero (z = 0). That is

$$z_i \sim \text{Bernoulli}\ (\psi).$$

The augmentation parameter ψ is a function of λ_s and the gamma noise term, η_s.

$$\psi = \frac{\sum_s \eta_s \lambda_s}{M}$$

The augmented data Y_i ($y_1, y_2 \ldots y_n$, 0, 0, … 0) with zero inflation can be modelled

conditional on the latent variables z_i.

$$Y_i \mid z_i=1 \sim \text{Binomial}\ (J, p)$$

$$Y_i \mid z_i = 0 \sim \delta\ (0).$$

To estimate the parameters, it is necessary to fix either a parameter of the gamma distribution (of the Gamma-Poisson mixed distribution) or the Bernoulli parameter ψ (see Converse and Royle, 2012).

Monte-Carlo simulations

We performed Monte Carlo simulations to evaluate the effectiveness of the hierarchical capture-recapture model. Because the model reliability has been confirmed (Tenan et al., 2017), we focused on 1) the effects of lowering detection probability and 2) the effects of heterogeneity in detection probability among animal passes or camera stations. We assumed that the number of detections by camera traps followed a negative binomial distribution with a mean of 5.0 and dispersion parameter 1.27, which deprived of the actual data on an ungulate in Nakashima et al. (2018). We also assumed two camera traps at 30 stations (i.e. 60 camera traps in total). We did not change these assumptions in the following scenarios.

In the first scenario, we evaluated the general model performance by assuming

a relatively high detection probability (0.8) without any random effects. In the second and third scenarios, the detection probability decreased to 0.5 (scenario 2) and 0.2 (scenario 3) without any random effects, respectively. In the fourth scenario, we made the detection probability heterogeneous among each animal pass, mimicking the situation in which camera sensitivity may depend on animal movements (e.g. walking speed). We assumed that the detection probability followed a normal distribution with a mean of 0.8 and an SD of 1.0 on the logit scale. In the fifth scenario, we tested the effects of random effects at camera station levels. We assumed that the detection probability varied among camera stations which followed a normal distribution with a mean of 0.8 and an SD of 1.0 on the logit scale. This may occur when the detection probability largely depends on the terrain or density of vegetation within the focal area.

In all the simulations, we estimated the model parameters using the Markov chain Monte Carlo (MCMC) implemented in JAGS (version 3.4.0). We constructed three models: a base model (without random effects), a model with station-specific random effects, and a model with animal pass-specific random effects. All three models were applied to the simulated data in all scenarios, and the parameters were estimated using the best-fit distribution based on the conditional WAIC value (Watanabe, 2010). In all scenarios, we assumed that the number of animal passes followed a negative

binomial distribution. Weakly informative prior, a gamma distribution with shape = 0.1 and rate = 0.1 was used for λ of negative binomial (Poisson-Gamma mixture) distributions and non-informative uniform distribution from 0 to 1 for the detection probability. The augmentation parameter ψ is estimated using a function of λ_s and the gamma noise term η_s. We generated three chains of 5000 iterations after a burn-in of 1000 and thinned by 5. The convergence of models was determined using the Gelman–Rubin statistic, where values <1.1 indicated convergence. These procedures were repeated 300 times. The JAGS code is available as supplementary material (Appendix 1).

Field surveys

We conducted a field survey in and around the Boumba-Bek and Nki National Parks in southeast Cameroon (October 2018 to January 2019) and the Boso Peninsula in Japan (August-November 2018). The study area of Cameroon consists primarily of evergreen and semi-deciduous forests (Letouzey, 1985). The annual rainfall is approximately 1,500 mm, and the mean annual temperature is 24.0°C (Nzooh Dongmo et al., 2016). Typically, the dry season occurs from December to February and the rainy season is from March to November. Information on mammalian fauna within the study site is

available from Hongo et al. (2020). The Boso Peninsula was in the southern part of Chiba Prefecture in central Japan (35N °N, 140E). The vegetation consists of either broad-leaved evergreen forests (*Castanopsis sieboldii* and *Quercus* spp.) or coniferous plantations (*Cryptomeria japonica* and *Chamaecyparis obtusa*). The monthly mean temperature was 20.6 ± 5.9 °C during the study period, with the highest in August (27.4 °C) and the lowest (13.6 °C) in November (Japan Meteorological Agency, 2019). The details of the study site are available from (Miyashita et al., 2008).

We used the same camera traps (Browning Strike Force Pro, BTC-5HDP, Browning, Missouri, US) at both study sites. This camera trap is reasonably priced (ca. 200 US dollars); it has a high trigger speed (< 1 s), and will be increasingly used for wildlife surveys. In Japan, we established 10 camera stations at least 2 km apart and installed two camera traps at each station. In Cameroon, we set 31 camera stations at least 2-km apart from each other. Following the approach proposed by Rowcliffe et al. (2013), we examined the frequency distribution of the distance from the camera to the location where the animals were first detected. This preliminary survey suggested that detection probability was highest within 1.0–3.5 m from the camera. We regarded an equilateral-triangle area (1.56 m^2) as the focal area (Fig. 1). We surrounded the focal area with a white rope and manually filmed it with camera traps as a reference. The rope

was removed after filming to avoid disturbing the animal behaviour. We set camera traps at approximately 0.7 m above ground without baits or lures. We used the ‘video mode’ and designated the video length as 20 s and the delay period between videos at 1 s (minimum delay period in this product).

We determined whether animals passed within or outside the focal area by superimposing videos and the reference image. We used only images of animals crossing the focal area for subsequent analyses. We then matched each detection from the two cameras to determine whether two camera traps at a station successfully recorded an animal pass. We performed the following two analyses. First, we applied the model to the detection probability of the species detected more than 10 times in both Japan and Cameroon. We considered the heterogeneity of animal passages and detection between the camera stations. The analysis was limited to images in which the animal species were reliably identified. Model parameters were estimated using the same procedure as in the Monte Carlo simulation (see above), and the best-fit model was selected based on conditional WAIC values. We plotted the estimated detection probability against the median value of body mass (kg), which was drawn from Ohdachi et al. (2009) for animals in Japan and Kingdon (2015) for those in Cameroon. Subsequently, we focused on the effect of the time of day on the detection probability of

the animals. While most animal species were captured only during a specific time of day, wild boar and muntjac were captured during both daytime and nighttime in Japan. For these two species, we incorporated the time of day (0: daytime, 1: nighttime) into the best-fit model of the first analysis as a covariate, defining daytime as 6:01-18:00 and nighttime as 18:01-6:00. We estimated the detection probability during the daytime and nighttime based on this model.

Results

Monte Carlo simulations

The results of the Monte Carlo simulations are presented in Table 1. The hierarchical capture-recapture model provided a good estimate of the detection probability and the number of animal passes with a reasonable confidence interval coverage when the detection probability was large (>0.5; ins. 1 and ins. 2). The model was also robust with respect to heterogeneous detection probabilities among animal passes and camera stations (ins. 4 and ins. 5). However, when the detection probability was set at 0.2 (. 3), there was overestimation by 57.9 ± 40.0 %, resulting in an underestimation of the number of animal passes by 25.8 ± 17.4 %.

Field surveys

Several camera traps (three in Japan and four in Cameroon) malfunctioned and did not provide animal images. The mean trapping effort was 82.3 ± 35.7 camera days (N = 7) in Japan while 30.1 ± 9.0 days (N = 26) in Cameroon. In total, 12 species were recorded more than 10 times (7 in Japan and 5 in Cameroon).

The analysis results for these species are summarised in Fig. 2 and Table S1 in the Supporting Information. Although none of the species was perfectly detected, the detection probability was relatively high (> 0.8) in all species except Japanese field mice (95% CI: 0.47 0.78. The detection probability did not vary significantly between the daytime and nighttime (Fig. 3). The 95 % credible interval of the time zone coefficient included 0 in both muntjac (95% CI: -1.355–0.576) and wild boar (95% CI: -1.446–0.643), indicating that there was no significant difference between daytime and nighttime.

Discussion

The field survey results showed that camera traps sometimes missed animals that passed through the focal area. Even for larger species, the detection probability did not reach 1 (Fig. 1, Table S1). Given that the size and position of the focal area were specified to

maximise the detection probability, the sensitivity of the camera model might be less than 1 throughout the detection zone. In previous studies, it was assumed that the detection probability would decrease with distance from the camera trap but must be certain at a given point near the camera trap (Rowcliffe et al., 2011). Fortunately, the results of our surveys suggest that the combination of a two-observer approach and a hierarchical capture-recapture model for a hierarchical population might be a practical approach to address this problem.

The results of the Monte Carlo simulation showed that the key to applying the approach reliably might be to secure a higher detection probability (> 0.5). In our field survey, the estimated detection probability was sufficiently high to use the model safely. Even for the field mice, the detection probability was not very low (95% CI: 0.47-0.78), suggesting that small mammals may be a potential target of our approaches. In practice, users need to set up camera traps carefully so as not to reduce the detection probability of target species. When two cameras face the same direction, the detection probability may be low away from the cameras. It may be better to discard images capturing animals at a distance from the camera before applying the models. If the cameras are installed in the opposite direction, as in our surveys, a more careful setting may be necessary because the detection probability may depend on the distance between

cameras. It is desirable to assess the area at which the detection probability is maximised, following Rowcliffe et al. (2011). Moreover, the detection probability may differ greatly between the centre and periphery of the camera's angle of view. Therefore, regardless of the camera direction, it may be critical to direct the two cameras to monitor exactly the same detection zone. Many recent camera models have built-in LCD monitors that allow the user to view the area being video-recorded in real-time. The use of these models may be required to set the cameras efficiently.

The field survey results also have important implications for estimating animal activity levels and the density of unmarked populations using camera traps. Fortunately, we showed that the detection probability of camera traps did not vary between daytime and nighttime in boar and muntjac in Japan. Although a large number of studies have relied on camera traps to assess animal activity levels, to the best of our knowledge, this is the first study to provide evidence of its validity. Given that detection probability may be largely dependent on environmental conditions, it may still be desirable to quantify the possible differences in other sites. In addition, the results of the surveys also suggest the need to refine current density estimation models relying on perfect detection (Rowcliffe et al., 2008; Howe et al., 2017; Campos-Candela et al., 2018; Moeller et al., 2018; Nakashima et al., 2018; Luo et al., 2020; Nakashima et al., 2020). In our surveys,

trapping rates were underestimated by 4 %–36%, which led directly to the underestimation of animal density by the same order of magnitude. Using a smaller focal area may be one possible way to reduce imperfect detection (Nakashima et al., 2018), but it would be more desirable to incorporate imperfect detection explicitly into the model. An advantage of the hierarchal capture-recapture model for stratified populations using the Bayesian framework is that it is easy to integrate into existing models. For example, one can use the parameter governing trapping rates (i.e. a parameter of the negative binomial distribution) as a part of the REST model (Nakashima et al., 2018). It is also relatively easy to incorporate distance sampling approaches and expand them to the distance capture-recapture model.

We admit that a shortcoming of this approach remains. In particular, it is necessary to have more cameras available, which may be a constraint on implementation. Nonetheless, researchers may be able to challenge these constraints in various ways. For example, it may not be necessary to install a pair of cameras at every camera station, as long as the variance in detection probability among camera stations is not too large. One may choose to install a pair of camera traps in locations with high trapping rates. If the detection probability is heterogeneous among camera stations, the study period may be divided into two parts: one in which two cameras are installed to

estimate the detection probability and one in which one camera is installed to estimate the trapping rate. Furthermore, if our approach were used at different locations, it would be possible to extrapolate the results to new sites by incorporating environmental conditions and animal characteristics as covariates. Given that many surveys estimating the density of marked populations use paired camera traps at each camera station (to recognise individual animals reliably), it may also be possible to roughly assess the detection probability from currently available data using the approach proposed here.

In this study, we showed that the double-observer approach, combined with hierarchical capture-recapture models using Bayesian frameworks, might be an effective option for estimating detection probabilities and the number of animal passes. We also suggest that commercially available camera traps can capture animals with a high probability of safely applying the capture-recapture model, at least in a small area of the camera detection zone. We believe that designating a focal area within the camera detection zone before the survey may be a simple way to avoid a high variation in detection probability among camera traps. Camera trappings have acquired an increasingly wider range of applications in animal ecology. For example, camera traps have been used to identify species that use a particular resource, such as fruits (e.g., (Nakashima et al., 2008) and carcasses (e.g., Peers et al., 2020). The approach proposed

here would be helpful for these studies (e.g. obtaining more reliable estimates of resource-use frequencies). We expect that the approach proposed here would make a wide range of camera-trapping studies more effective.

Acknowledgements

This study complied with the Republic of Cameroon laws. It was conducted with approval from the Ministry of Scientific Research and Innovation (MINRESI, N°0190/ MINRESI/Projet COMECA/PM/07/2018) and the Ministry of Forestry and Wildlife (MINFOF, N°1527/L/MINFOF/SETAT/SG/DFAP/SDCF/SEP/EP), Cameroon. This study was financially supported by JST/JICA SATREPS (JPMJSA1702) and JSPS KAKENHI Grant Number 15K07487.

Authors' contributions

YN conceived the ideas and designed the methodology; SH and YG collected the data; KM and YG performed video analyses; YN wrote the manuscript. All authors contributed critically to the drafts and approved the final manuscript for publication.

Data archive statement

We intend to archive all data used in this study at the Dryad.

References

Alldredge, M.W., Pollock, K.H., & Simons, T.R. (2006). Estimating detection probabilities from multiple-observer point counts. *The Auk, 123,* 1172-1182. https://doi.org/10.1093/auk/123.4.1172

Apps, P., & McNutt, J.W. (2018). Are camera traps fit for purpose? A rigorous, reproducible and realistic test of camera trap performance. *African Journal of Ecology, 56,* 710-720. https://doi.org/10.1111/aje.12573

Burton, A.C. (2012). Critical evaluation of a long-term, locally-based wildlife monitoring program in West Africa. *Biodiversity and conservation, 21,* 3079-3094. https://doi.org/10.1007/s10531-012-0355-6

Campos-Candela, A., Palmer, M., Balle, S., Alós, J., & Gaillard, J.M. (2018). A camera-based method for estimating absolute density in animals displaying home range behaviour. *Journal of Animal Ecology, 87,* 825-837. https://doi.org/10.1111/1365-2656.12787

Chandler, R.B., & Royle, J.A. (2013). Spatially explicit models for inference about density in unmarked or partially marked populations. *The Annals of Applied Statistics, 7,* 936-954. https://doi.org/10.1214/12-AOAS610

Damm, P.E., Grand, J.B., & Barnett, S.W. (2010). Variation in detection among passive

infrared triggered-cameras used in wildlife research. *Proceedings of the Annual Conferece of Southeast Associations of Fish and Wildlife Agencies, 64,* 125-130.

Driessen, M.M., Jarman, P.J., Troy, S., & Callander, S. (2017). Animal detections vary among commonly used camera trap models. *Wildlife Research, 44,* 291-297. https://doi.org/10.1071/WR16228

Findlay, M.A., Briers, R.A., & White, P.J. (2020). Component processes of detection probability in camera-trap studies: understanding the occurrence of false-negatives. *Mammal Research, 65,* 167-180. https://doi.org/10.1007/s13364-020-00478-y

Gardner, B., Reppucci, J., Lucherini, M., & Royle, J.A. (2010). Spatially explicit inference for open populations: estimating demographic parameters from camera-trap studies. *Ecology, 91,* 3376-3383. https://doi.org/10.1890/09-0804.1

Gilbert, N.A., Clare, J.D., Stenglein, J.L., & Zuckerberg, B. (2021). Abundance estimation methods for unmarked animals with camera traps. *Conservation Biology, 35,* 88-100. https://doi.org/10.1111/cobi.13517

Hofmeester, T.R., Cromsigt, J.P.G.M., Odden, J., Andrén, H., Kindberg, J., & Linnell, J.D.C. (2019). Framing pictures: A conceptual framework to identify and correct for biases in detection probability of camera traps enabling multi-species

comparison. *Ecology and Evolution, 9,* 2320-2336. https://doi.org/10.1002/ece3.4878

Hongo, S., Dzefack, Z.S.C., Vernyuy, L.N., Minami, S., Nakashima, Y., Djiéto-Lordon, C., & Yasuoka, H. (2020). Use of multi-layer camera trapping to inventory mammals in rainforests in southeast Cameroon. *African study monographs, 60,* 21-37. https://doi.org/10.14989/250126

Howe, E.J., Buckland, S.T., Després-Einspenner, M.L., & Kühl, H.S. (2017). Distance sampling with camera traps. *Methods in Ecology and Evolution, 8,* 1558-1565. https://doi.org/10.1111/2041-210X.12790

Jacobs, C.E., & Ausband, D.E. (2018). An evaluation of camera trap performance–What are we missing and does deployment height matter? *Remote Sensing in Ecology and Conservation, 4,* 352-360. https://doi.org/10.1002/rse2.81

Japan Meteorological Agency (2020). https://www.data.jma.go.jp/gmd/risk/obsdl/index.php (Accessed April 2, 2021).

Karanth, K.U. (1995). Estimating tiger *Panthera tigris* populations from camera-trap data using capture-recapture models. *Biological Conservation, 71,* 333-338. https://doi.org/10.1016/0006-3207(94)00057-W

Kingdon, J. (2015). *The Kingdon field guide to African mammals (2nd ed.).* Bloomsbury

Publishing, London.

Kissling, M.L., & Garton, E.O. (2006). Estimating detection probability and density from point-count surveys: a combination of distance and double-observer sampling. *The Auk, 123,* 735-752. https://doi.org/10.1642/0004-8038(2006)123[735:EDPADF]2.0.CO;2

Letouzey, R. (1985). *Carte Phytogéographique du Cameroun au 1:500000. Institut de la Recherche Agronomique (Herbier National).* Toulouse, France.

Li, X., Bleisch, W.V., & Jiang, X. (2018). Using large spatial scale camera trap data and hierarchical occupancy models to evaluate species richness and occupancy of rare and elusive wildlife communities in southwest China. *Diversity and Distributions, 24,* 1560-1572. https://doi.org/10.1111/ddi.12792

Linkie, M., Dinata, Y., Nugroho, A., & Haidir, I.A. (2007). Estimating occupancy of a data deficient mammalian species living in tropical rainforests: sun bears in the Kerinci Seblat region, Sumatra. *Biological Conservation, 137,* 20-27. https://doi.org/10.1016/j.biocon.2007.01.016

Luo, G., Wei, W., Dai, Q., & Ran, J. (2020). Density estimation of unmarked populations using camera traps in heterogeneous space. *Wildlife Society Bulletin, 44,* 173-181. https://doi.org/10.1002/wsb.1060

MacKenzie, D.I., Nichols, J.D., Royle, J.A., Pollock, K.H., Bailey, L., & Hines, J.E. (2017). *Occupancy estimation and modeling: inferring patterns and dynamics of species occurrence*. New York, NY: Academic Press. https://doi.org/10.1016/C2012-0-01164-7

McIntyre, T., Majelantle, T., Slip, D., & Harcourt, R. (2020). Quantifying imperfect camera-trap detection probabilities: implications for density modelling. *Wildlife Research, 47,* 177-185. https://doi.org/10.1071/WR19040

Miyashita, T., Suzuki, M., Ando, D., Fujita, G., Ochiai, K., & Asada, M. (2008). Forest edge creates small-scale variation in reproductive rate of sika deer. *Population Ecology, 50,* 111–120. https://10.1007/s10144-007-0068-y

Moeller, A.K., Lukacs, P.M., & Horne, J.S. (2018). Three novel methods to estimate abundance of unmarked animals using remote cameras. *Ecosphere, 9,* e02331. https://doi.org/10.1002/ecs2.2331

Nakashima, Y. (2015). Inventorying medium-and large-sized mammals in the African lowland rainforest using camera trapping. *Tropics, 23,* 151-164. https://doi.org/10.3759/tropics.23.151

Nakashima, Y., Fukasawa, K., & Samejima, H. (2018). Estimating animal density without individual recognition using information derivable exclusively from

camera traps. *Journal of Applied Ecology, 55,* 735-744. https://doi.org/10.1111/1365-2664.13059

Nakashima, Y., Hongo, S., & Akomo-Okoue, E.F. (2020). Landscape-scale estimation of forest ungulate density and biomass using camera traps: Applying the REST model. *Biological Conservation, 241,* 108381. https://doi.org/10.1016/j.biocon.2019.108381

Nakashima, Y., Lagan, P., & Kitayama, K. (2008). A study of fruit–frugivore interactions in two species of durian (*Durio*, Bombacaceae) in Sabah, Malaysia. *Biotropica, 40,* 255-258. https://doi.org/10.1111/j.1744-7429.2007.00335.x

Nichols, J.D., Hines, J.E., Sauer, J.R., Fallon, F.W., Fallon, J.E., & Heglund, P.J. (2000). A double-observer approach for estimating detection probability and abundance from point counts. *The Auk, 117,* 393-408. https://doi.org/10.1093/auk/117.2.393

Norouzzadeh, M.S., Nguyen, A., Kosmala, M., Swanson, A., Palmer, M.S., Packer, C., & Clune, J. (2018). Automatically identifying, counting, and describing wild animals in camera-trap images with deep learning. *Proceedings of the National Academy of Sciences, 115,* E5716-E5725. https://doi.org/10.1073/pnas.1719367115

Nzooh Dongmo, Z., K.P. N'goran, G. Etoga, J.P. Belinga, E. Fouda, M. Dandjouma, &

P. Dongmo (2016). *Les populations de grandes et moyens mammifères dans le segment Cameroun du paysage TRIDOM (forêt de Ngoyla-Mintom, et PN Boumba Bek et PN Nki et leurs zones périphériques).* Ministère des Forêts et de la Faune and WWF Cameroon Country Programme Office, Cameroon.

Ohdachi, S.D., Ishibashi, Y., Iwasa, M.A., Saitoh, T. (2009). *The wild mammals of Japan.* Shoukadon Book Sellers, Kyoto.

Peers, M.J., Konkolics, S.M., Lamb, C.T., Majchrzak, Y.N., Menzies, A.K., Studd, E.K., Boonstra, R., Kenney, A.J., Krebs, C.J., & Martinig, A.R. (2020). Prey availability and ambient temperature influence carrion persistence in the boreal forest. *Journal of Animal Ecology, 89,* 2156-2167. https://doi.org/10.1111/1365-2656.13275

Ramsey, D.S., Caley, P.A., & Robley, A. (2015). Estimating population density from presence–absence data using a spatially explicit model. *The Journal of Wildlife Management, 79,* 491-499. https://doi.org/10.1002/jwmg.851

Randler, C., & Kalb, N. (2018). Distance and size matters: A comparison of six wildlife camera traps and their usefulness for wild birds. *Ecology and Evolution, 8,* 7151-7163. https://doi.org/10.1002/ece3.4240

Riddle, J.D., Pollock, K.H., & Simons, T.R. (2010). An unreconciled double-observer

method for estimating detection probability and abundance. *The Auk, 127,* 841-849. https://doi.org/10.1525/auk.2010.09118

Rovero, F., Martin, E., Rosa, M., Ahumada, J.A., & Spitale, D. (2014). Estimating species richness and modelling habitat preferences of tropical forest mammals from camera trap data. *PLoS One,* 9, e103300. https://doi.org/10.1371/journal.pone.0103300

Rovero, F., Zimmermann, F., Berzi, D., & Meek, P. (2013). "Which camera trap type and how many do I need?" A review of camera features and study designs for a range of wildlife research applications. *Hystrix, 24,* 148-156. https://doi.org/10.4404/hystrix-24.2-8789

Rowcliffe, J.M., Carbone, C., Jansen, P.A., Kays, R., & Kranstauber, B. (2011). Quantifying the sensitivity of camera traps: an adapted distance sampling approach. *Methods in Ecology and Evolution, 2,* 464-476. https://doi.org/10.1111/j.2041-210X.2011.00094.x

Rowcliffe, J.M., Field, J., Turvey, S.T., & Carbone, C. (2008). Estimating animal density using camera traps without the need for individual recognition. *Journal of Applied Ecology, 45,* 1228-1236. https://doi.org/10.1111/j.1365-2664.2008.01473.x

Royle, J.A., & Dorazio, R.M. (2008). *Hierarchical modeling and inference in ecology: the analysis of data from populations, metapopulations and communities*. New York, NY: Academic Press. https://doi.org/10.1016/B978-0-12-374097-7.50001-5

Royle, J.A., Nichols, J.D., Karanth, K.U., & Gopalaswamy, A.M. (2009). A hierarchical model for estimating density in camera-trap studies. *Journal of Applied Ecology, 46,* 118-127. https://doi.org/10.1111/j.1365-2664.2008.01578.x

Silveira, L., Jacomo, A.T., & Diniz-Filho, J.A.F. (2003). Camera trap, line transect census and track surveys: a comparative evaluation. *Biological Conservation, 114,* 351-355. https://doi.org/10.1016/S0006-3207(03)00063-6

Sollmann, R., Mohamed, A., Samejima, H., & Wilting, A. (2013). Risky business or simple solution–Relative abundance indices from camera-trapping. *Biological Conservation, 159,* 405-412. https://doi.org/10.1016/j.biocon.2012.12.025

Suryawanshi, K.R., Bhatnagar, Y.V., & Mishra, C. (2012). Standardizing the double-observer survey method for estimating mountain ungulate prey of the endangered snow leopard. *Oecologia, 169,* 581-590. https://doi.org/10.1007/s00442-011-2237-0

Tabak, M.A., Norouzzadeh, M.S., Wolfson, D.W., Sweeney, S.J., VerCauteren, K.C.,

Snow, N.P., Halseth, J.M., Di Salvo, P.A., Lewis, J.S., & White, M.D. (2019). Machine learning to classify animal species in camera trap images: Applications in ecology. *Methods in Ecology and Evolution, 10,* 585-590. https://doi.org/10.1111/2041-210X.13120

Tenan, S., Brambilla, M., Pedrini, P., & Sutherland, C. (2017). Quantifying spatial variation in the size and structure of ecologically stratified communities. *Methods in Ecology and Evolution, 8,* 976-984. https://doi.org/10.1111/2041-210X.12719

Tobler, M.W., Carrillo-Percastegui, S.E., & Powell, G. (2009). Habitat use, activity patterns and use of mineral licks by five species of ungulate in south-eastern Peru. *Journal of Tropical Ecology*, 261-270. https://doi.org/10.1017/S0266467409005896

Tobler, M.W., Zúñiga Hartley, A., Carrillo‐Percastegui, S.E., & Powell, G.V. (2015). Spatiotemporal hierarchical modelling of species richness and occupancy using camera trap data. *Journal of Applied Ecology, 52,* 413-421. https://doi.org/10.1111/1365-2664.12399

Watanabe, S. (2010). Asymptotic equivalence of bayes cross validation and widely applicable information criterion in singular learning theory

. *Journal of Machine Learning Research, 11*, 3571–3594.

Willi, M., Pitman, R.T., Cardoso, A.W., Locke, C., Swanson, A., Boyer, A., Veldthuis, M., & Fortson, L. (2019). Identifying animal species in camera trap images using deep learning and citizen science. *Methods in Ecology and Evolution, 10,* 80-91. https://doi.org/10.1111/2041-210X.13099

Figure legends

Fig. 1. A schematic diagram showing the installation of cameras at a station. Two cameras were installed at each station to monitor the same focal area. The focal area is an equilateral triangle with a side of 1.9 m, and the distance from the camera to the nearest vertex is 1.65 m. The camera used (Browning Strike Force Pro) has a sensor detection range of about 42°, and the semi-transparent triangle in the diagram indicates the area of the detection zone.

Fig. 2. The estimated detection probability of 12 species within a small focal area (XX m^2) in Cameroon (5 species) and Japan (7 species) using the capture-recapture models for stratified populations. Error bar shows the 95% credible interval.

Fig. 3. The estimated detection probability of muntjac and wild boars during daytime and night-time. Error bar shows the 95% credible interval.

Figure

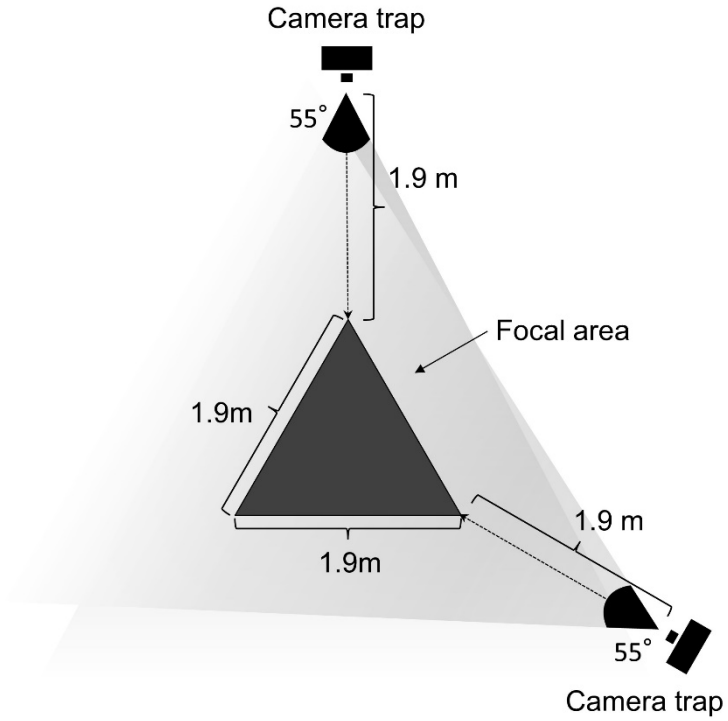

Fig. 1

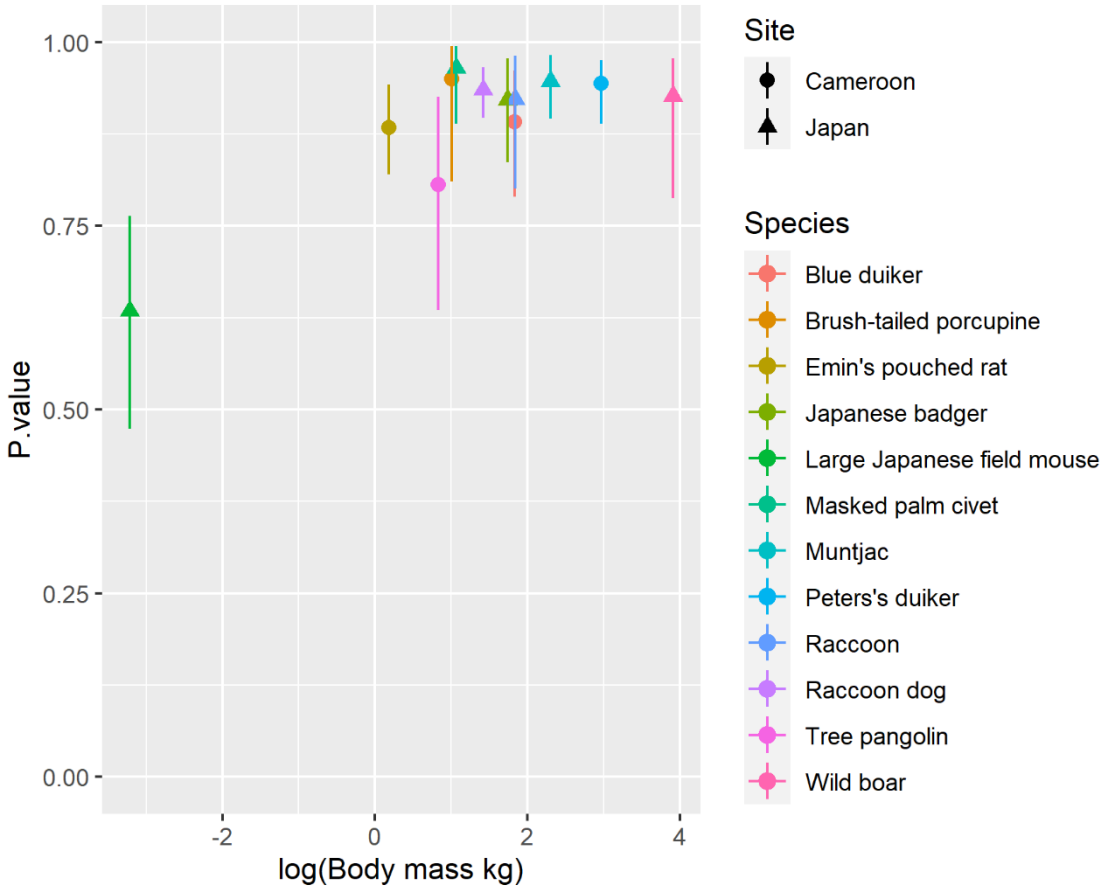
1.00
0.75
0.50
0.25
0.00
P.value
-2
0
2
4
log(Body mass kg)
Site
Cameroon
Japan
Species
Blue duiker
Brush-tailed porcupine
Emin's pouched rat
Japanese badger
Large Japanese field mouse
Masked palm civet
Muntjac
Peters's duiker
Raccoon
Raccoon dog
Tree pangolin
Wild boar

Fig. 2

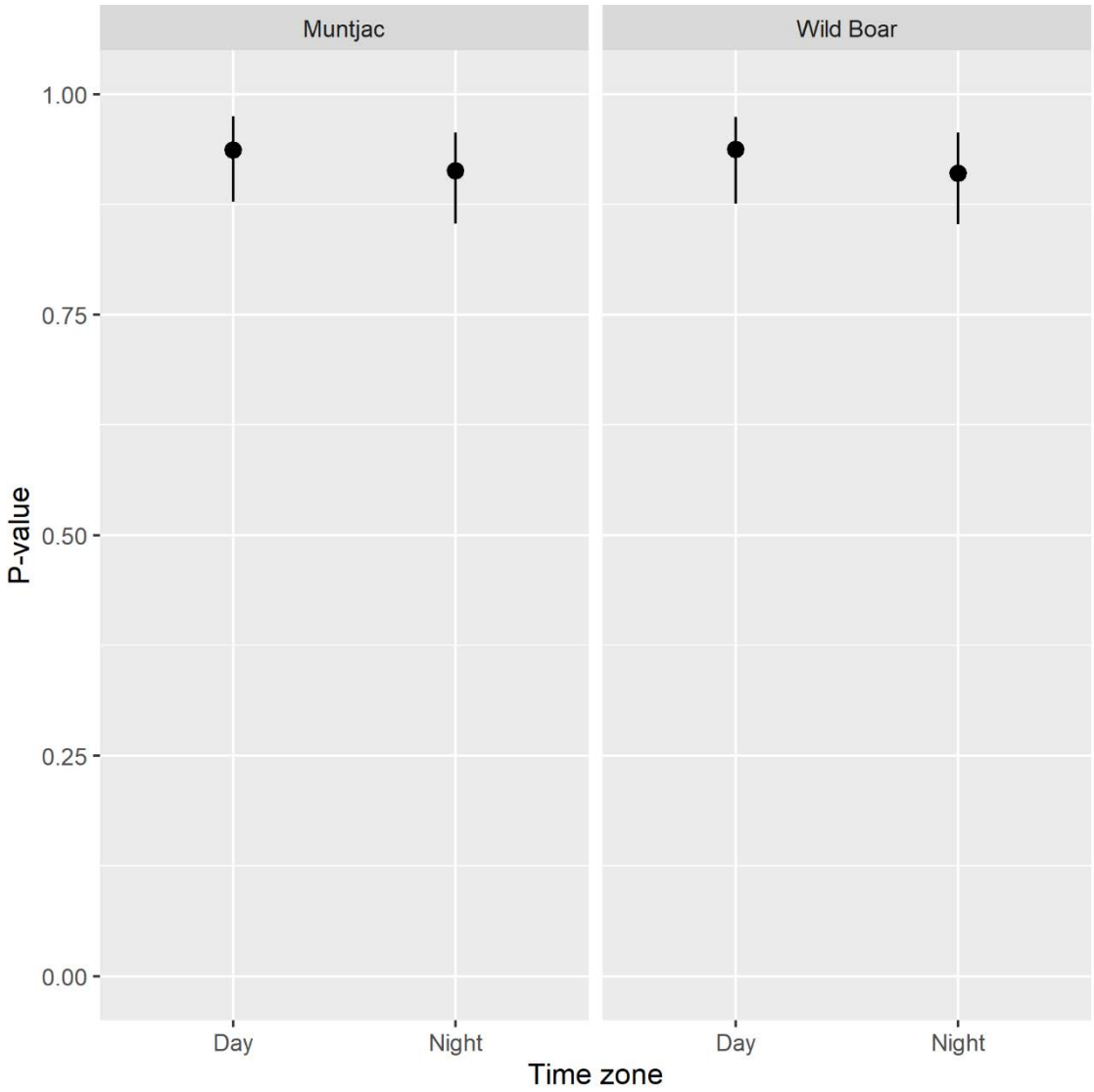
Muntjac
Wild Boar
1.00
0.75
0.50
0.25
0.00
P-value
Day
Night
Day
Night
Time zone

Fig. 3

Table

Table 1. Summary of the Monte Carlo simulations. Results are the number of successful fits of the hierarchical CR models (N) among the 300 iterations, the number of times that each of the three models (base model without random effects, random passage model, and random site model) was selected based on the conditional WAIC value, the mean and median of estimated detection probability P and the expected number of animal passes (lambda), and their 95% credible interval (CI) coverage of the densities. Parameter estimation of the CR model was performed using the Markov chain Monte Carlo (MCMC) method, and their variances and credible limits were calculated as the posterior summary.

ID	*N*	Best-fit models			*P*			*lambda*		
		Base	Random pass	Random site	Mean	Median	CI Coverage (%)	Mean	Median	CI Coverage (%)
Scenario 1	300	229	4	67	0.80	0.80	0.95	5.04	5.02	0.93
Scenario 2	300	272	14	14	0.51	0.51	0.96	5.00	4.96	0.88

Scenario 3	300	241	48	11	0.27	0.26	0.62	3.71	3.68	0.46
Scenario 4	300	118	118	64	0.80	0.80	0.96	5.27	5.23	0.92
Scenario 5	300	197	8	95	0.80	0.80	0.89	5.00	4.91	0.91

Supplementary material

Table S1. Summary of the applications of the hierarchical capture-recapture model to the field data in Japan and Cameroon. Results are the number of the animal passes detected (N) the best-fit model based on the conditional WAIC value (Base: base model without random effects; Site: site-specific random effects; Pass: animal's pass specific random effects), the mean and median of estimated detection probability P and the expected number of animal passes (lambda), and their 95% credible interval. Parameter estimation of the capture-recapture model was performed using the Markov chain Monte Carlo (MCMC) method, and their variances and credible limits were calculated as the posterior summary. Body mass (kg) was adapted from Kingdon et al. (2015) or Ohdachi et al. (2009).

			Body mass		Best-fit	*P*			*lambda*		
Site	Species	Scientific name	(kg)	*N*	model	Median	95% CI		Median	95% CI	
Cameroon	Blue duiker	*Philantomba monticola*	6.3	78	Site	0.89	0.79 -	0.96	11.96	7.00 -	16.21
	African brush-tailed porcupine	*Atherurus africanus*	2.8	13	Site	0.94	0.77 -	0.99	9.13	5.15 -	11.88

	Emin's pouched rat	*Cricetomys emini*	1.2	140	Site	0.89	0.82	-	0.94	9.62	7.42	-	14.13
	Peters's duiker	*Cephalophus callipygus*	19.5	54	Pass	0.96	0.91	-	0.99	6.05	3.66	-	14.35
	Tree pangolin	*Phataginus tricuspis*	2.3	24	Site	0.80	0.64	-	0.92	9.55	8.27	-	10.49
Japan	Wild boar	*Sus scrofa*	50.0	407	Pass	0.92	0.78	-	0.98	28.87	21.03	-	40.64
	Japanese Badger	*Meles anakuma*	5.7	78	Pass	0.92	0.83	-	0.98	30.29	16.74	-	46.78
	Large Japanese field mouse	*Cricetomys emini*	0.0	279	Site	0.64	0.47	-	0.78	15.43	13.39	-	22.32
	Masked palm civet	*Paguma larvata*	2.9	61	Pass	0.96	0.89	-	0.99	30.57	13.91	-	73.87
	Muntjac	*Muntiacus reevesi*	10.0	133	Pass	0.95	0.90	-	0.98	26.60	10.98	-	72.37
	Raccoon	*Procyon lotor*	6.3	52	Pass	0.92	0.81	-	0.98	34.70	10.24	-	141.84
	Raccoon dog	*Nyctereutes procyonoides*	4.1	200	Pass	0.94	0.90	-	0.97	45.58	27.15	-	93.04

Appendix 1. R code to perform the Monte-Carlo simulations to test the reliability of hierarchical capture-recapture models for stratified population to estimate detection probability and correct potentially imperfect detection.

```
library(MASS);library(jagsUI);library(loo);library(tidyverse)

nsim<-300 # Number of iteration
nstation<-30 # Number of camera stations
ncamera<-2 # Number of cameras at a station
lambda<-5 # Parameter for trapping rate
theta<-1.27 # Dispersion parameter for trapping rate
basep<-0.8 # Parameter for detection probability

base_waic<-pass_waic<-site_waic<-numeric(0)
neg_base_p<-neg_pass_p<-neg_site_p<-neg_base_lambda<-neg_pass_lambda<-
        neg_site_lambda<-list(0)

simn<-0
for(m in 1:nsim){
  simn<-simn+1
  cat(paste(simn,", ",sep=""))

  npass_station<-rnegbin(nstation,lambda, theta=theta)
  npass_total<-sum(npass_station)
  station_pass<-rep(1:nstation,npass_station)

  # Random effects at animal pass levels
  logit.basep <- log((basep)/(1-(basep)))
  prob.p<-1/(1 + exp(- logit.basep - rnorm(npass_total,0,1)))

  # Random effects at camera station levels
  logit.basep <- log((basep)/(1-(basep)))
```

```
prob.station<-1/(1 + exp(- logit.basep - rnorm(nstation,0,1)))
prob.s <- rep(prob.station,npass_station)

# Base model without random effects
prob.b<-rep(basep,npass_total)

y.full <- rbinom(npass_total, prob=prob.b, ncamera) # Base model
y <- y.full[y.full!=0]

w<- c(y,rep(0,length(y)*1.5))
M<-length(w)
Q<-length(y)
V<-station_pass[y.full!=0]

g<-c(V,rep(NA,M-Q))
K<-ncamera
datalist <- list(w=w,nstation=nstation,M=M,K=K,g=g, Q=Q)

# Base model --------

model<-"C:¥¥bugstemp¥¥model_HCR_NB.txt"
sink(model)
cat("
   model {
   p ~ dunif(0,1)
   alpha ~ dnorm(0,0.1)
   psi <- sum(omega[])/M # ~ dunif(0,1)
   a ~ dunif(0,1000)
   b ~ dunif(0,1000)

   for(s in 1:nstation){
      eta[s] ~ dgamma(a,a)
      log(lam[s])<-alpha
      omega[s]<-eta[s]*lam[s]
      gprobs[s]<-omega[s]/sum(omega[])
```

```
        }
        temp<-lam[1]
        for(i in 1:M){
            g[i] ~ dcat(gprobs[])
            z[i] ~ dbern(psi)
            w[i]~ dbin(mu[i],K)
            mu[i] <- z[i]*p
            lik_base[i]<-log(gprobs[g[i]]*dbin(w[i],mu[i],K))
        }
        }
        ",fill=TRUE)
    sink()
    inits <- function()list(z=rep(1,M))
    parameters <- c("p","psi","temp","mu","lik_base","gprobs")
    n.chain<-3;n.iter<-5000;n.burnin<-1000;n.thin<-5
    nmcmc<-n.chain*(n.iter-n.burnin)/n.thin
    neg_base <-jags(datalist, inits, parameters, model,
                            n.chain=n.chain,n.iter=n.iter,n.burnin=n.burnin,n.thin=n.thin,
            parallel=TRUE)

    lik_base <- matrix(0,byrow=T,ncol=M,nrow=nmcmc)

    psi<-neg_base$sims.list$psi
    p<-neg_base$sims.list$p
    N<-neg_base$sims.list$N
    mu<-neg_base$sims.list$mu
    gprobs<-neg_base$sims.list$gprobs

    (base_waic[m]<-waic(neg_base$sims.list$lik_base)$estimates[3,1])

    neg_base_p[[m]]<-c(neg_base$q50$p,neg_base$q2.5$p,neg_base$q97.5$p)
    neg_base_lambda[[m]]<-
            c(neg_base$q50$temp,neg_base$q2.5$temp,neg_base$q97.5$temp)
```

```
# Random pass model --------

model<-"C:¥¥bugstemp¥¥model_HCR_NB.txt"

sink(model) #model の前にクォーテーションが必要

cat("
   model {
   alpha ~ dnorm(0,0.1)
   psi <- sum(omega[])/M # ~ dunif(0,1)
   a ~ dunif(0,1000)
   mean ~ dnorm(0,0.1)
   tau ~ dgamma(0.1,0.1)

   for(s in 1:nstation){
      eta[s] ~ dgamma(a,a)
      log(lam[s])<-alpha
      omega[s]<-eta[s]*lam[s]
      gprobs[s]<-omega[s]/sum(omega[])
   }
   temp<-lam[1]

   for(i in 1:M){
      g[i] ~ dcat(gprobs[])
      z[i] ~ dbern(psi)
      w[i]~ dbin(mu[i],K)
      mu[i] <- z[i]*p[i]
      logit(p[i]) <- beta0[i]
      beta0[i] ~ dnorm(mean,tau)
      lik_pass[i]<-log(gprobs[g[i]]*dbin(w[i],mu[i],K))
   }
   }
   ",fill=TRUE)
sink()
```

```
inits <- function()list(z=rep(1,M))
parameters <- c("temp","p","psi","mu","mean","lik_pass","gprobs")
neg_pass <-jags(datalist, inits, parameters, model,
                        n.chain=n.chain,n.iter=n.iter,n.burnin=n.burnin,n.thin=n.thin,
      parallel=TRUE)
psi<-neg_pass$sims.list$psi
mu<-neg_pass$sims.list$mu
N<-neg_pass$sims.list$N
gprobs<-neg_pass$sims.list$gprobs

(pass_waic[m]<-waic(neg_pass$sims.list$lik_pass)$estimates[3,1])

neg_pass_p[[m]]<-1/(1+exp(-
      c(neg_pass$q50$mean,neg_pass$q2.5$mean,neg_pass$q97.5$mean)))
neg_pass_lambda[[m]]<-
      c(neg_pass$q50$temp,neg_pass$q2.5$temp,neg_pass$q97.5$temp)

# Negative Binomial/ b    fixed/ random site --------

model<-"C:¥¥bugstemp¥¥model_HCR_NB.txt"


sink(model)
cat("
   model {
   alpha ~ dnorm(0,0.1)
   psi <- sum(omega[])/M # ~ dunif(0,1)
   a ~ dunif(0,1000)
   mean ~ dnorm(0,0.1)
   tau ~ dgamma(0.1,0.1)
   theta ~ dgamma(0.1,0.1)

   for(s in 1:nstation){
      eta[s] ~ dgamma(a,a)
      log(lam[s])<-alpha
```

```
            omega[s]<-eta[s]*lam[s]
            gprobs[s]<-omega[s]/sum(omega[])
        }
        temp<-lam[1]

        for(i in 1:M){
            g[i] ~ dcat(gprobs[])
            z[i] ~ dbern(psi)
            w[i] ~ dbin(mu[i],K)
            mu[i] <- z[i]*p[i]
            logit(p[i]) <- beta0[g[i]]
            lik_site[i]<-log(gprobs[g[i]]*dbin(w[i],mu[i],K))
        }
        for(i in 1:nstation){
            beta0[i] ~ dnorm(mean,tau)
        }
        }
        ",fill=TRUE)
    sink()
    inits <- function()list(z=rep(1,M))
    parameters <- c("temp","p","psi","mu","mean","lik_site","gprobs")
    neg_site <-jags(datalist, inits, parameters, model,
                            n.chain=n.chain,n.iter=n.iter,n.burnin=n.burnin,n.thin=n.thin,
            parallel=TRUE)
    psi<-neg_site$sims.list$psi
    p<-neg_site$sims.list$mu
    N<-neg_site$sims.list$N
    gprobs<-neg_site$sims.list$gprobs

    (site_waic[m]<-waic(neg_site$sims.list$lik_site)$estimates[3,1])

    neg_site_p[[m]]<-1/(1+exp(-
            c(neg_site$q50$mean,neg_site$q2.5$mean,neg_site$q97.5$mean)))
    neg_site_lambda[[m]]<-
            c(neg_site$q50$temp,neg_site$q2.5$temp,neg_site$q97.5$temp)
```

```
}

par(mfrow=c(2,2))
par(mar=c(3, 4, 3, 2) + 0.1)
par(mgp=c(2.2, 1, 0))

lam.base<-do.call(rbind,neg_base_lambda)
lam.pass<-do.call(rbind,neg_pass_lambda)
lam.site<-do.call(rbind,neg_site_lambda)

plot(1:nsim,lam.base[,1],ylim=c(0,10),main="base")
segments(1:nsim,lam.base[,2],1:nsim,lam.base[,3],col=1)
lines(c(-1,nsim*2),c(lambda,lambda),lty=2)
plot(1:nsim,lam.pass[,1],ylim=c(0,10),main="pass")
segments(1:nsim,lam.pass[,2],1:nsim,lam.pass[,3],col=2)
lines(c(-1,nsim*2),c(lambda,lambda),lty=2)
plot(1:nsim,lam.site[,1],ylim=c(0,10),main="site")
segments(1:nsim,lam.site[,2],1:nsim,lam.site[,3],col=3)
lines(c(-1,nsim*2),c(lambda,lambda),lty=2)

p.base<-do.call(rbind,neg_base_p)
p.pass<-do.call(rbind,neg_pass_p)
p.site<-do.call(rbind,neg_site_p)

plot(1:nsim,p.base[,1],ylim=c(0,1),main="base")
segments(1:nsim,p.base[,2],1:nsim,p.base[,3],col=1)
lines(c(-1,nsim*2),c(basep,basep),lty=2)
plot(1:nsim,p.pass[,1],ylim=c(0,1),main="pass")
segments(1:nsim,p.pass[,2],1:nsim,p.pass[,3],col=2)
lines(c(-1,nsim*2),c(basep,basep),lty=2)
plot(1:nsim,p.site[,1],ylim=c(0,1),main="site")
segments(1:nsim,p.site[,2],1:nsim,p.site[,3],col=3)
lines(c(-1,nsim*2),c(basep,basep),lty=2)

par(mfrow=c(2,1))
```

```
df<-data.frame(base_waic,pass_waic,site_waic)
min.col<-apply(as.matrix(df),1,which.min)
lam_50<-lam_25<-lam_75<-numeric(0)
for(i in 1:nsim){
   lam_50[i]<-data.frame(lam.base[,1],lam.pass[,1],lam.site[,1])[i,min.col[i]]
   lam_25[i]<-data.frame(lam.base[,2],lam.pass[,2],lam.site[,2])[i,min.col[i]]
   lam_75[i]<-data.frame(lam.base[,3],lam.pass[,3],lam.site[,3])[i,min.col[i]]
}
plot(1:nsim,lam_50,ylim=c(0,10),main="Best R")
segments(1:nsim,lam_25,1:nsim,lam_75,col=min.col)
lines(c(-1,nsim*2),c(lambda,lambda),lty=2)

p_50<-p_25<-p_75<-numeric(0)
for(i in 1:nsim){
   p_50[i]<-data.frame(p.base[,1],p.pass[,1],p.site[,1])[i,min.col[i]]
   p_25[i]<-data.frame(p.base[,2],p.pass[,2],p.site[,2])[i,min.col[i]]
   p_75[i]<-data.frame(p.base[,3],p.pass[,3],p.site[,3])[i,min.col[i]]
}
plot(1:nsim,p_50,ylim=c(0,1),main="Best R")
segments(1:nsim,p_25,1:nsim,p_75,col=min.col)
lines(c(-1,nsim*2),c(basep,basep),lty=2)
############################
neg_base<-neg_pass<-neg_site<-NULL

#save.image("HCR_STR.RData")
```